New Reflector Shaping Methods for Dual-Reflector Antenna

Kamelia QUZWAIN [1,2], Yoshihide YAMADA [1], Kamilia KAMARDIN [1], Nurul Huda ABD RAHMAN [3], Alyani ISMAIL [4]

[1] Malaysia-Japan International Institute of Technology, Universiti Teknologi Malaysia, Kuala Lumpur 54100, Malaysia
[2] Institut Teknologi Telkom Jakarta, West Jakarta 11710, Indonesia
[3] Universiti Teknologi MARA, Shah Alam, Selangor 40450 , Malaysia
[4] Faculty of Engineering, Universiti Putra Malaysia, Selangor 43400, Malaysia

kquzwain77@gmail.com, yoshide@utm.my, kamilia@utm.my, nurulhuda0340@uitm.edu.my, alyani@upm.edu.my

Submitted April 11, 2021 / Accepted September 16, 2021

Abstract. *In the fifth-generation (5G) mobile system, new millimeter-wave technologies such as small cell size and multibeam operation are introduced at the base station. Currently, the hybrid beam forming array antennas are developed for beam steering operations. However, the array antenna configuration has drawback of increased feed circuit loss and antenna gain reduction. Moreover, many modulation/demodulation circuits increase the antenna price. The reflector antenna is another option for multi beam operations that has high gain and small feeder loss. The problem of the reflector antenna is how to achieve good multi beam radiation patterns. Previously, reflector shaping method of the dual reflector antenna was proposed. However, previous method can't apply for good multi beam designing. In this paper, modification to the reflector shaping method using equivalent parabola reflector and equivalent circle reflector method is proposed to achieve a good multi beam radiation patterns. First, the equivalent parabola and circle equation is implemented in the reflector shaping algorithms. Second, a Matrix Laboratory (MATLAB) program is developed in order to obtain the main and sub reflector shapes. The accuracy of MATLAB program is ensured from the obtained ray path results, aperture distribution and radiation pattern. In the final step, multi beam performance is validated using an electromagnetic simulator, FEKO. Through comparison of the equivalent parabola with the equivalent circle reflectors, an antenna efficiency of 67.6% is obtained and better multi beam radiation patterns are demonstrated using the equivalent circle reflector. Therefore, the usefulness of the newly developed shaping method employing equivalent circle reflector is ensured.*

Keywords

Dual reflector antenna, reflector shaping method, equivalent parabola reflector, equivalent circle reflector, ray tracing method

1. Introduction

Nowadays, 5G mobile systems are rapidly developed to achieve fast rate transmission, low latency, extremely high traffic volume density, super-dense connections and improved spectral energy, as well as cost efficiencies [1–5]. With the introduction of 5G, the radio technology has new features such as millimeter wave operation, small cell size and multi beam base station antenna to meet the massive Multi-Input-Multi-Output (MIMO) requirement [2], [3]. For this purpose, the hybrid beam forming array antenna (employing the digital beam forming technology (DBF)) has been developed to be used at base stations in the urban areas as shown in Fig. 1(a). In the case of large number of array element, feeding circuit loss will be increased and the antenna gain will be decreased. Moreover, large number of modulation/demodulation circuits attached at the array elements will increase the antenna price. So, the hybrid beam forming array antenna will be suitable at the high population area such as the urban area. For the rural areas where less population and less beams are required, a lower-cost solution of high gain antenna will be suitable. The reflector type antenna has a feature of low loss and achieving high gain. The multi beam radiation patterns can be easily achieved by placing many feed horns as shown in Fig. 1(b). However, the antenna design method of achieving good multi beam radiation patterns was not made clear.

Previous well known antenna design method was the reflector shaping technique that was developed to achieve high gain at the on-focus feed of the dual-reflector antenna [6]. Through the reflector shaping, the constant phase and adequate amplitude distributions were achieved on the antenna aperture plane.

The reflector shaping method was composed of three differential equations. The two differential equations were for the reflection condition on the main and sub reflectors. The third differential equation represents electrical power conservation law from the feed to the antenna aperture plane. These simultaneous three differential equations were

DOI: 10.13164/re.2022.0039

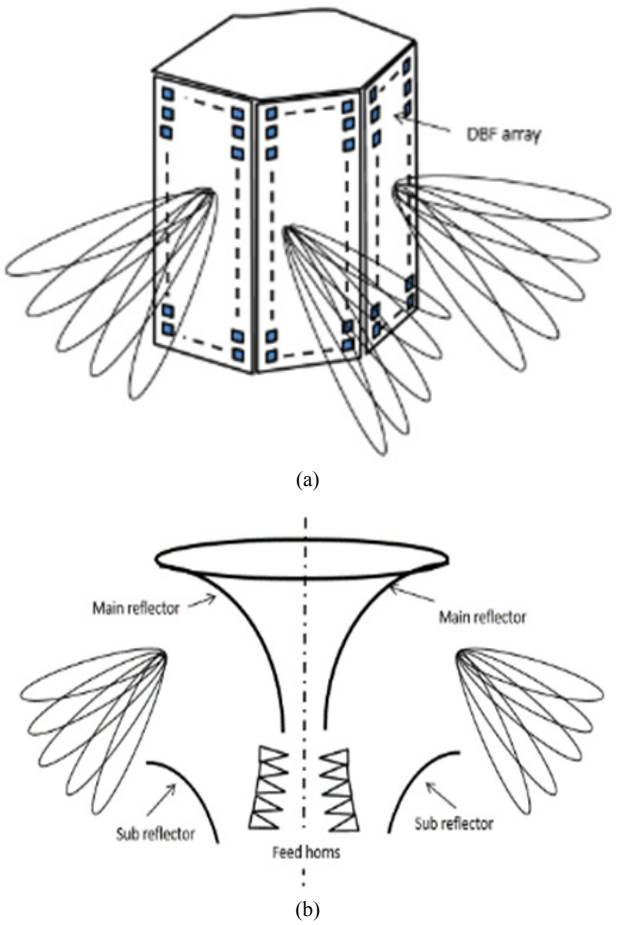

Fig. 1. (a) Digital Beam Forming (DBF) antenna for base stations and (b) the proposed reflector antenna system for base stations.

solved numerically at the given parameters of horn radiation pattern and the target aperture distribution [6]. Although the target aperture distribution was obtained, ability for multi beam performance was not expected.

For the purpose of achieving good multi beam radiation patterns, the spherical reflector antenna was proposed. Due to the symmetrical structure around the spherical center, good multi beam radiation pattern were obtained by employing off-focus feeds [7]. However, the spherical aberration degrades the phase distribution on the aperture plane and thus causes serious reduction in antenna gain. If the previously developed reflector shaping method can be applied to the spherical reflector structure, the constant phase can be achieved on the spherical reflector configuration.

In this paper, the modification of reflector shaping method is proposed in order to mitigate phase aberration of the spherical reflector antenna. The idea of modifying the reflector shaping method comes from the equivalent parabola concept of the Cassegrain dual reflector antenna in [8]. During modification, first, the third differential equation is replaced by the equivalent parabola equation. Based on the successful replacement, the equivalent circle equation is applied for the third equation. Second, in order to ensure the accuracy of the proposed method, the reflector shaping program is developed using MATLAB software. By the developed program, the expected pencil beam width and high gain can be achieved through the proposed equivalent concepts. Through the ray tracing results, the designed reflector shapes, aperture distribution and radiation pattern can be obtained and thus, the reliability and accuracy of the technique are ensured. In order to validate the designed antenna, a full-wave electromagnetic analysis is obtained by FEKO simulator. It is shown that the excellent multibeam and moderate antenna gain can be achieved by the proposed antenna.

2. Reflector Shaping Equations

The modification processes are done based on the conventional reflector shaping method. The equivalent parabola and circle reflector concepts are employed during the modification of equations and it is explained in this section.

2.1 Conventional Shaping Method

The configuration and parameters that are related to the conventional reflector shaping method are shown in Figs. 2(a) and (b), respectively. The dual reflector shaping method was formed by three differential equations composed of two differential equations for the main and sub reflectors and another differential equation that expresses electric power conservation between a feed radiation and aperture distribution. Two reflection equations and one electric power conservation equation are expressed as follows [6].

a) Reflection law on the sub reflector

The reflection condition on the sub reflector surface is given by the next equation. Here, r is the ray length from the feed to the sub reflector, θ is feed angle and ϕ is the reflected ray angle on the sub reflector.

$$\frac{\mathrm{d}r}{\mathrm{d}\theta} = r\tan\frac{\theta+\phi}{2}. \tag{1}$$

b) Reflection law on the main reflector

All reflected rays from the main reflector are set parallel to the horizontal axis. Afterwards, plane waves are produced in front of the main reflector. The constant phase distribution is achieved on the aperture plane. The reflection condition on main reflector surface can be determined by the next equation.

$$\frac{\mathrm{d}z}{\mathrm{d}\theta} = \frac{\mathrm{d}x}{\mathrm{d}\theta}\tan\frac{\phi}{2}. \tag{2}$$

c) Electric power conservation

The relation of electric power conservation can be written as:

$$\frac{\mathrm{d}x}{\mathrm{d}\theta}=\frac{E_p^2(\theta)\int_0^{x_m}E_d^2(x)\mathrm{d}x}{E_d^2(x)\int_0^{\theta_m}E_p^2(\theta)\mathrm{d}\theta} \tag{3}$$

where $E_p^2(\theta)$ is an electric field intensity of the feed antenna and $E_d^2(x)$ is the aperture distribution.

d) Equality of ray path length

The differential equations (1) and (2) are expressed by a variable θ. In solving differential equations with a variable θ, ϕ should be expressed by θ. The following constant equation for the electrical path length (l_z) is used to obtain the relation of θ and ϕ.

$$L_{\mathrm{T}}=r_0+\frac{R_{\mathrm{M}}-R_{\mathrm{S}}}{\sin\phi_{\mathrm{M}}}+\frac{R_{\mathrm{M}}}{\tan\phi_{\mathrm{M}}}. \tag{4}$$

The relation for θ and ϕ is given by the equation.

$$x=l_1\sin\phi+r\sin\theta \tag{5}$$

where l_1 is ray length from the sub reflector to the main reflector.

The three simultaneous differential equations composed of (1), (2) and (3) can be solved by using MATLAB software.

e) $E_p^2(\theta)$ and $E_d^2(x)$ expressions

The radiation pattern of the feed antenna is given in a simplified form as shown by (6) [6]:

$$E_p^2(\theta)=\cos^q(\theta). \tag{6}$$

Here, the q-value is selected to achieve the main reflector edge level of –10 dB.

The amplitude distribution of $E_d^2(x)$ and $E_p^2(\theta)$ play a key role in dual reflector shaping. According to the law of energy conservation, the relation between $E_d^2(x)$ and $E_p^2(\theta)$ can be written as [6]:

$$\Delta\theta E_p^2(\theta)=\Delta x E_d^2(x) \tag{7}$$

where Δx is the ray spacing at the aperture plane and $\Delta\theta$ is the ray spacing of the feed.

2.2 Modification of Reflector Shaping Method by the Equivalent Parabola Reflector

The dual reflector antenna configuration of Fig. 2 (Cassegrain antenna) can be replaced by the equivalent parabola shown in Fig. 3. By using x-coordinate equation at the equivalent parabola, $\mathrm{d}x/\mathrm{d}\theta$ of (3) will be replaced by a new equation.

In Fig. 3, the equivalent parabola represented by the dashed line at a certain distance f_e from the feed can achieve the equivalent electric performance as the dual reflector. For a given feed angle θ, the radial coordinates x of the equivalent parabola is expressed by the next equation:

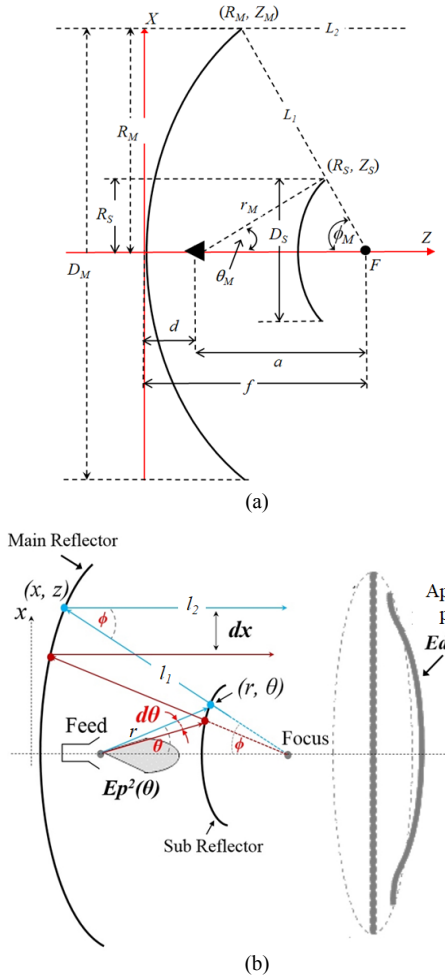

Fig. 2. (a) Structural parameters and (b) relation between angle and electric power of the conventional reflector shaping method.

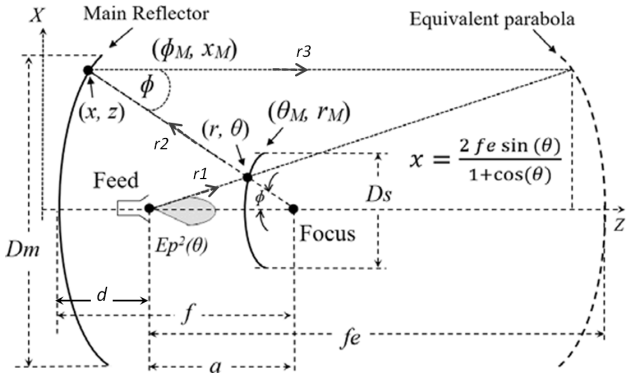

Fig. 3. Equivalent parabola shaping method.

$$x=\frac{2f_{\mathrm{e}}\sin\theta}{1+\cos\theta}. \tag{8}$$

The differential form of (8) can be expressed as follows:

$$\frac{\mathrm{d}x}{\mathrm{d}\theta}=2f_{\mathrm{e}}\left\{\frac{\sin\theta^2}{(1+\cos\theta)^2}+\frac{\cos\theta}{1+\cos\theta}\right\}=\frac{2f_{\mathrm{e}}}{1+\cos\theta} \tag{9}$$

where f_e indicates the equivalent parabolic focal length.

Therefore, the electric power conservation of (3) can be replaced by (9). The new set of differential equations represented by (1), (2) and (9) become the modified version of the dual reflector shaping equations. These three simultaneous differential equations are expressed by one variable θ. So, the solution can be obtained by using MATLAB software. By the equivalent parabola shaping method, the result of reflector is expected to be a Cassegrain reflector antenna.

The f_e value can be expressed in terms of eccentricity value e as follows [9]:

$$f_e = \frac{e+1}{e-1} f. \tag{10}$$

The eccentricity e is expressed as follows:

$$e = \frac{\sin\left(\frac{\phi+\theta}{2}\right)}{\sin\left(\frac{\phi-\theta}{2}\right)}. \tag{11}$$

2.3 Modification of Reflector Shaping Method by the Equivalent Circle Reflector

Based on the successful modification of reflector shaping method by the equivalent parabola reflector, the equivalent parabola equation can be further improved. In reference to the purpose of designing a spherical reflector, an equivalent circle reflector is considered.

The equivalent circle reflector concept is shown in Fig. 4. By this concept, the main and sub reflectors are supposed to be replaced by the equivalent circle reflector which is shown by the dashed line. The radius of the circle reflector is denoted as f_c. On the equivalent circle reflector, the relation of x and θ is expressed by the next equation:

$$x = f_c \sin\theta. \tag{12}$$

The differential form of (12) is written as follows:

$$\frac{dx}{d\theta} = f_c \cos\theta \tag{13}$$

where f_c is given by the next expression:

$$f_c = \frac{R_M}{\sin\theta}. \tag{14}$$

In this case, Equation (13) is used to replace the electric power conservation in (3). The new set of differential equations that are composed of (1), (2) and (13) is the modified version of the dual reflector shaping equations. These three simultaneous differential equations are expressed by one variable θ and it can be solved by using MATLAB software. The result of reflector is expected similar to the spherical reflector by using the equivalent circle shaping method.

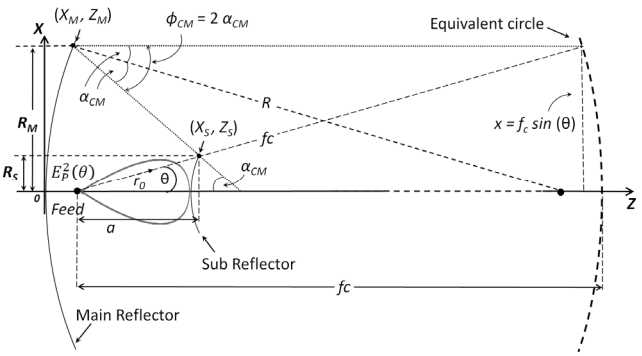

Fig. 4. Equivalent circle shaping method.

3. MATLAB Program

In order to solve the three simultaneous differential equations, a computation program was developed using Matrix Laboratory (MATLAB) software. The concept of the developed MATLAB program is shown in Fig. 5. In the MATLAB program, many designed results such as designed reflector shapes, ray tracing, aperture distribution and radiation pattern are shown. The program is developed in the following manner. Firstly, the initial values of antenna structure are set. The second step is to calculate reflector surfaces based on the three equations. The third step is drawing calculation results such as reflector shapes, ray racing, aperture distribution and radiation pattern.

3.1 Conventional Reflector Shaping Method

The purpose of developing a MATLAB program for the conventional reflector shaping method is to ensure the accuracy of the developed program. Based on the structural parameters as shown in Fig. 2(a), the initial calculation parameters are shown in Tab. 1. The diameter of the main reflector can be calculated by the next equation [10]:

$$\frac{D_M}{f} = 4\tan\left(\frac{\Phi_M}{2}\right). \tag{15}$$

Here f is the focal length and Φ_M is the main reflector angle.

The feed radiation pattern is shown in Fig. 6. The q-value of the feed pattern $E_p^2(\theta)$ given by (6) is determined to achieve the sub reflector edge level of –10 dB. The q-value is set to be 37 for the feed angle θ_f of 20 degree.

For the aperture distribution $E_d^2(x)$, Equation (16) is used:

$$E_d^2(x) = \left[1.1 - \left(\frac{x}{x_{max}}\right)\right]^p. \tag{16}$$

Here, x_{max} is the maximum position of the main reflector. The parameter p determines the strength of the aperture distribution taper.

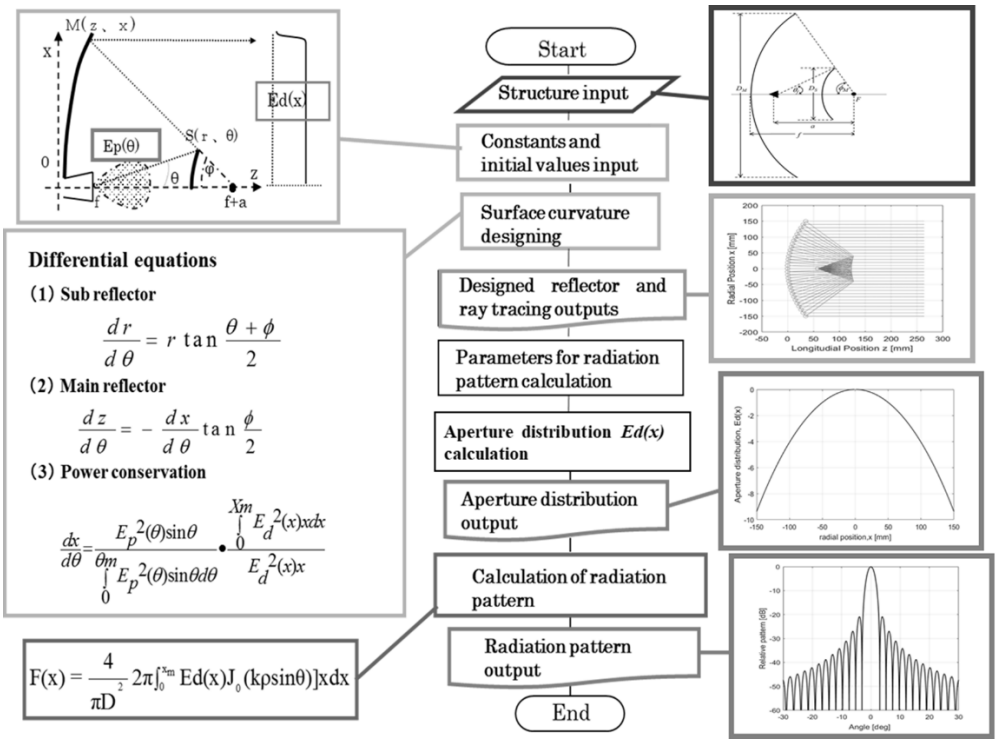

Fig. 5. Function of developed MATLAB program.

Parameters	Value	Unit
Frequency (*Freq.*)	28	GHz
Diameter of main reflector (D_M)	300	mm
Diameter of sub reflector (D_S)	60	mm
Main reflector focal length (f)	120	mm
Main reflector angle (ϕ_M)	70	degree
Distance between focus point and feed (a)	93.3	mm
Feed angle (θ_f)	20	degree

Tab. 1. Initial parameters for conventional reflector shaping method.

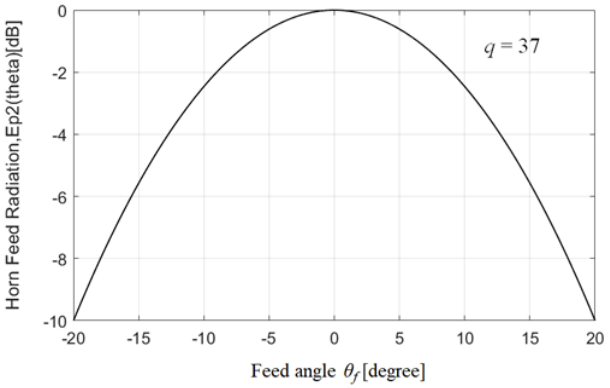

Fig. 6. Feed pattern of $E_p^2(\theta)$.

The aperture distributions of $p = 0$ and $p = 1$ are shown in Fig. 7(a) and (b), respectively. $p = 0$ achieves the uniform aperture distribution that is suitable for checking the program accuracy by comparing the theoretical value.

By using $E_p^2(\theta)$ and $E_d^2(x)$ of Fig. 6, the reflector shapes are designed by the developed MATLAB program. Reflector shapes for $p = 0$ and $p = 1$ are shown in Figs. 8(a) and (b), respectively. The ray tracing result shows that all

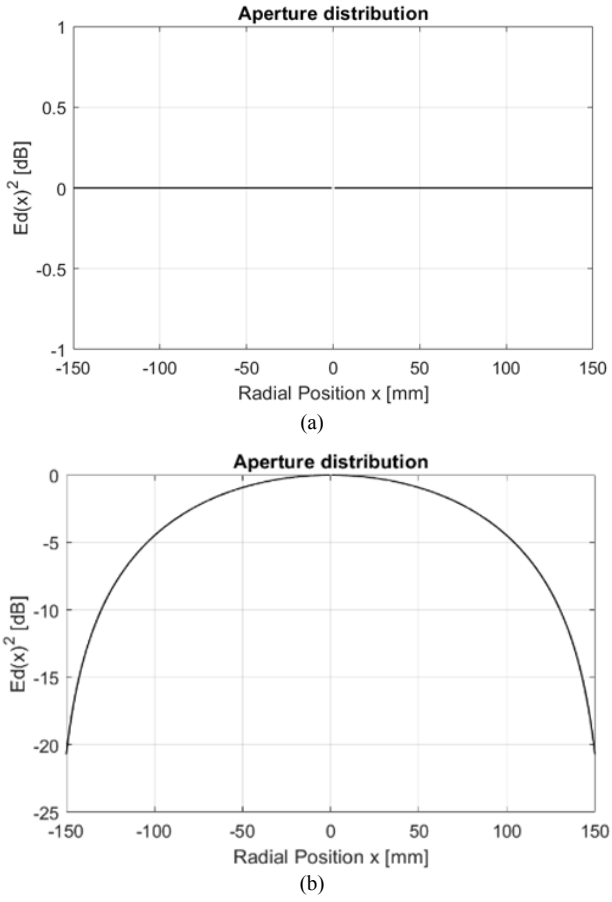

Fig. 7. The aperture distribution of $E_d^2(x)$ for (a) $p = 0$ and (b) $p = 1$.

rays in front of the main reflector become parallel to the horizontal axis. The parallel characteristics mean that the

constant phase distribution is achieved on the aperture plane. From the ray separation of Fig. 8(a), it can be observed that the ray separation at the reflector edge becomes very narrow compared to the reflector center.

The ray separation change depends on the energy conservation law in (7). In order to compensate the power reduction of $E_p^2(\theta)$, the ray separation (Δx) becomes narrow till the reflector edge. In the case of Fig. 8(b), in order to achieve the sharp taper of Fig. 7(b) from the loose taper of Fig. 6, the ray separation at the edge becomes sparse compared to the reflector center. From the ray tracing results, the adequateness of the developed MATLAB program is ensured.

The radiation pattern can be calculated by the next equation [9]:

$$E_R(\theta) = 2\pi \int_0^{x_{\max}} E_d(x) J_0(kx\sin\theta)\,\mathrm{d}x. \qquad (17)$$

Here, k is the wave number and J_0 indicates the Bessel function of the first kind.

The calculated radiation patterns for $p = 0$ and $p = 1$ are shown in Fig. 8. The dotted and the solid lines correspond to the value of $p = 0$ and $p = 1$, respectively. It can be observed that the first side lobe level (*SLL*) of the uniform aperture distribution is –17.5 dB that agrees with the theoretical value of –17.6 dB [9]. The *SLL* of the tapered distribution is –24.4 dB that agrees with the theoretical value of –24.6 dB [9].

As a result, from the ray tracing results and radiation results, the performance of the developed MATLAB program is verified to be accurate.

3.2 Proposed Reflector Shaping Method by Equivalent Parabola

In order to ensure the adequateness of the proposed equivalent parabola method, the designed results by the developed MATLAB program are examined. The structural parameters of Fig. 3 structure are shown in Tab. 2.

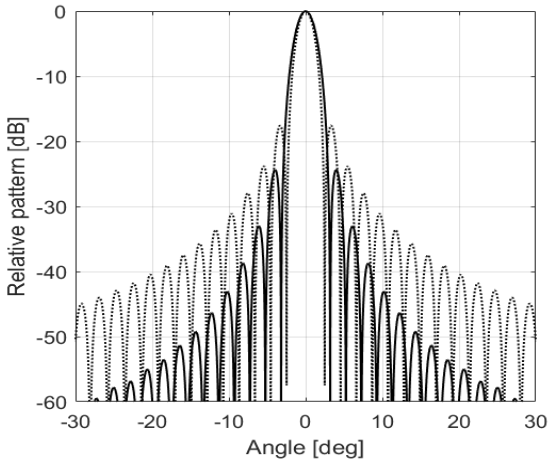

Fig. 8. Radiation patterns for $p = 0$ (dotted) and $p = 1$ (solid).

Parameters	Value	Unit
Frequency (*Freq.*)	28	GHz
Diameter of main reflector (D_M)	300	mm
Diameter of sub reflector (D_S)	80	mm
Equivalent parabola focal length (f_e)	280	mm
Focal length (f)	160.8	mm
Main reflector angle (ϕ_M)	50	degree
Feed position (d)	58	mm
Distance between focus point and feed (a)	102.8	mm
Feed angle (θ_M)	30	degree

Tab. 2. Structural parameters of the equivalent parabola method.

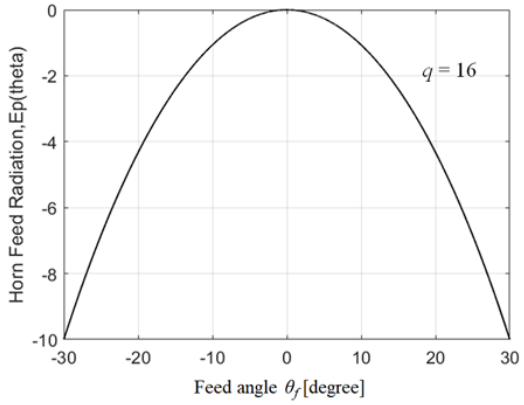

Fig. 9. Feed radiation pattern of $E_p^2(\theta)$.

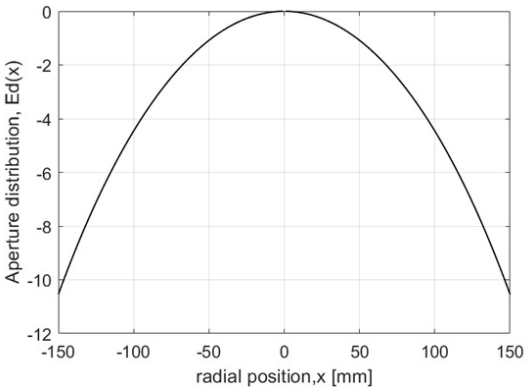

Fig. 10. The aperture illumination distribution $E_d^2(x)$.

The feed radiation pattern $E_p^2(\theta)$ as shown in Fig. 9 given by (6) is determined to achieve the sub reflector edge level of –10 dB. For $\theta_f = 30$ degree, q becomes 16.

The aperture distribution $E_d^2(x)$ is determined by $E_p^2(\theta)$ that is shown (7):

$$E_d^2(x) = E_p^2(\theta)\frac{\mathrm{d}\theta}{\mathrm{d}x} = \cos(\theta)^q(1+\cos\theta). \qquad (18)$$

The obtained aperture distribution is shown in Fig. 10.

The designed reflector shapes and ray tracing results are shown in Fig. 11. It can be observed that all rays become parallel to the z-axis after reflection on the main reflector. The parallel rays mean that uniform phase distribution is achieved on the antenna aperture plane as the ray separation becomes constant. The ray separation change depends on the energy conservation law in (7). In this case,

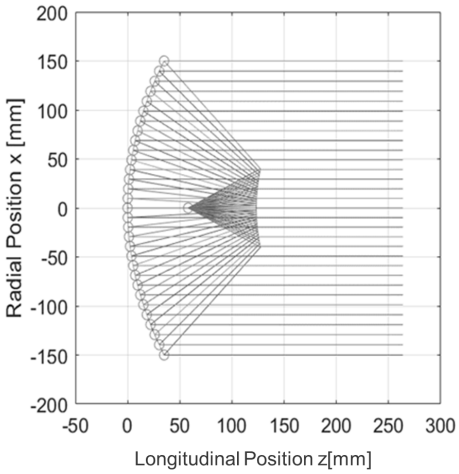

Fig. 11. The ray tracing result of equivalent parabola method.

as the tapering of Fig. 10 and Fig. 11 becomes almost similar where Δx is similar to $\Delta\theta$ which is constant. From the ray tracing results as shown in Fig. 11, the adequateness of the reflector shaping method is shown.

Next, the reflector shapes are examined. By the equivalent parabola reflector method, the Cassegrain antenna is designed. In the Cassegrain antenna case, the main reflector surface point (x,z) is given by the next equation [9], [11]:

$$x^2 = 4fz. \tag{19}$$

The hyperbola sub reflector structure is shown in Fig. 12. By the eccentricity value e, the sub reflector shape becomes hyperbola or ellipse as shown by (20) [9], [11]:

$$e = \frac{c}{b}\begin{cases} > 1 \text{ hyperbola} \\ < 1 \text{ ellipse} \end{cases} \tag{20}$$

The hyperbola sub reflector surface (x_s, z_s) is expressed by (21) [9], [11]:

$$\frac{z_s^2}{b^2} - \frac{x_s^2}{c^2 - b^2} = 1. \tag{21}$$

From Tab. 2, f is 160.8 mm and $c = a/2$ is 51.4 mm while b variable is set to be 13.9 mm. Table 3 shows the comparison results of the designed and theoretical coordinates. It can be observed that the designed main and sub reflectors agree with the parabola and hyperbola, respectively. It is concluded that the Cassegrain antenna is designed accurately by the equivalent parabola reflector method.

Figure 13 demonstrates the radiation pattern of the designed dual reflector antenna. It shows that the *SLL* is

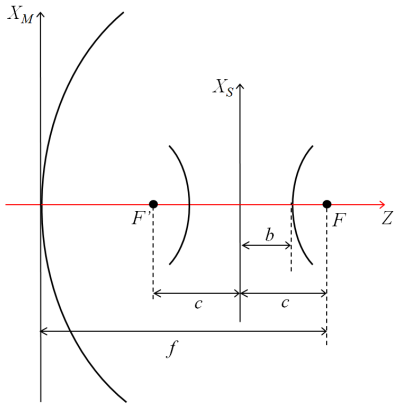

Fig. 12. Hyperbola sub reflector structure.

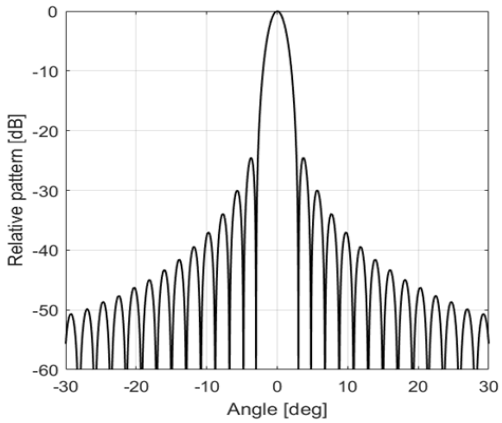

Fig. 13. 2-D radiation pattern of the equivalent parabola.

–24.5 dB and the half power beam width (*HPBW*) is 2.7 degree. By taking into account the aperture distribution of Fig. 10 that has the edge level of –10.5 dB, the first side lobe level is adequate.

3.3 Proposed Reflector Shaping Method by Equivalent Circle

In the previous subsection, the equivalent parabola equation can be applied successfully to the conventional reflector shaping method. From the result, the Cassegrain antenna that has a parabolic main reflector is achieved.

In this sub section, the parabola equation is replaced by the equivalent circle equation and applied to the conventional reflector shaping method. The designed main reflector shape is expected to be similar to the spherical reflector. Table 4 lists the initial calculation parameters for MATLAB program based on the Fig. 4.

θ (deg)	Main Reflector (mm)				Sub Reflector (mm)			
	Designed		Theoretical Parabola		Designed		Theoretical Hyperbola	
	X_m	Z_m	X_m	Z_m	X_s	Z_s	X_s	Z_s
30	150	35	150	35	40	127.3	40	127.3
20	98.8	15.2	98.9	15.2	24.4	124.9	24.3	124.8
10	49	3.7	49	3.7	11.6	123.7	11.5	123.7
0	0	0	0	0	0	123.3	0	123.3

Tab. 3. Comparison results between designed and theoretical coordinates.

Parameters	Value	Unit
Frequency (*Freq.*)	28	GHz
Diameter of main reflector (D_M)	300	mm
Diameter of sub reflector (D_S)	80	mm
Equivalent parabola focal length (f_e)	300	mm
Main reflector angle (ϕ_M)	50	degree
Feed position (d)	34.4	mm
Distance between focus point and feed (a)	69.3	mm
Feed angle (θ_f)	30	degree

Tab. 4. Initial parameters of the equivalent circle method.

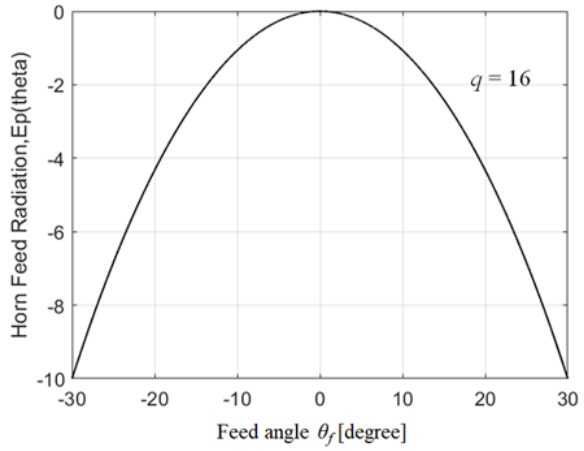

Fig. 14. Feed pattern of $E_p^2(\theta)$ for equivalent circle.

In Fig. 14, the feed radiation pattern is shown. The radiation pattern is determined to achieve the sub reflector edge level of –10 dB at $\theta_f = 30$ degree. The q value of (6) becomes 16.

By using the electric power conservation relation between $E_p^2(\theta)$ and $E_d^2(x)$ of (7) and applying the relation of (13), the aperture distribution can be expressed by (22):

$$E_d^2(x) = E_p^2(\theta)\frac{\mathrm{d}\theta}{\mathrm{d}x} = \cos(\theta)^{(q-1)}. \qquad (22)$$

The obtained aperture distribution is shown in Fig. 15. The edge level becomes –9.37 dB. By comparing the Fig. 15 result with the equivalent parabola case of Fig. 10, the edge level of the equivalent circle case is increased 1 dB than the equivalent parabola case.

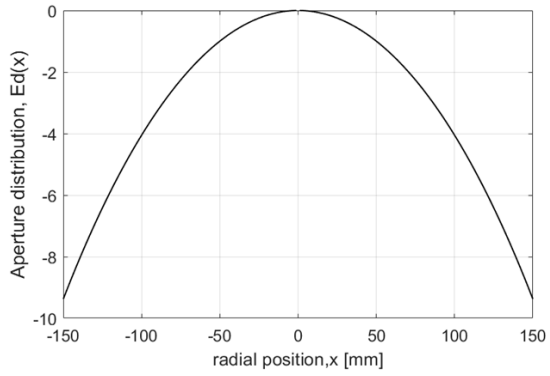

Fig. 15. The aperture distribution $E_d^2(x)$ of the equivalent circle.

The ray tracing result is shown in Fig. 16. When comparing reflector shapes with Fig. 11 result, a slight difference is observed at the sub reflector shapes. The ray separations Δx on the antenna aperture become almost constant since the designed step angle $\Delta\theta$ is constant.

The comparison of the main reflector shape and the spherical reflector shape is shown in Tab. 5. At the reflector edge of $x_m = 150$ mm, z_m values of the designed shape and the sphere become 40.2 and 35.6 mm. The difference is a very small value of 4.6 mm. At $x_m = 103.8$ mm and 51.8 mm, z_m values become the same. So, the designed main reflector is very similar to the spherical reflector. In order to make clear the difference of the main reflector shapes, the ray tracing results at the focal region are compared in Fig. 17. In the case of Fig. 17(a), the focal region rays converge at the focus point. However, in the case of the spherical reflector case shown in Fig. 17(b), the focal region rays do not converge at one point [12]. By checking the focal region rays, the difference of reflectors are clear. As a conclusion of this section, the proposed equivalent circle method can achieve semi spherical main reflector that has a constant phase distribution on the aperture plane. Therefore, high gain and good multibeam radiation patterns are expected.

The radiation pattern of the equivalent circle reflector is shown in Fig. 18. The *SLL* and the beamwidth are –20.8 dB and 2.4 degree, respectively. In comparison with Fig. 13 of the equivalent parabola case, the *SLL* is increased around 4 dB. The increase in the *SLL* depends on the incre-

θ (deg)	Main Reflector (mm)				Sub Reflector (mm)	
	Designed		Spherical Shape		Designed	
	X_m	Z_m	X_m	Z_m	X_s	Z_s
30	150	40.2	150	35.6	40	103.7
20	103.8	18.5	103.7	18.5	24.6	101.1
10	51.8	16.5	51.7	16.5	11.4	99.5
0	0	0	0	0	0	99

Tab. 5. Comparison results between main reflector shape and the spherical shape.

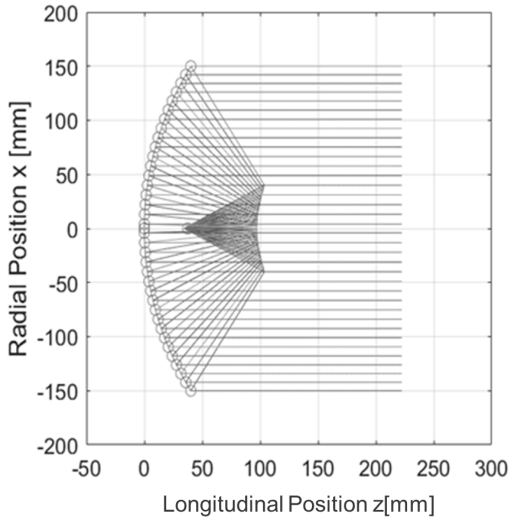

Fig. 16. The ray tracing of the equivalent circle.

ment of aperture edge level shown in Fig. 15 as compared to Fig. 10. Then, in the equivalent circle case, an antenna gain increase is expected.

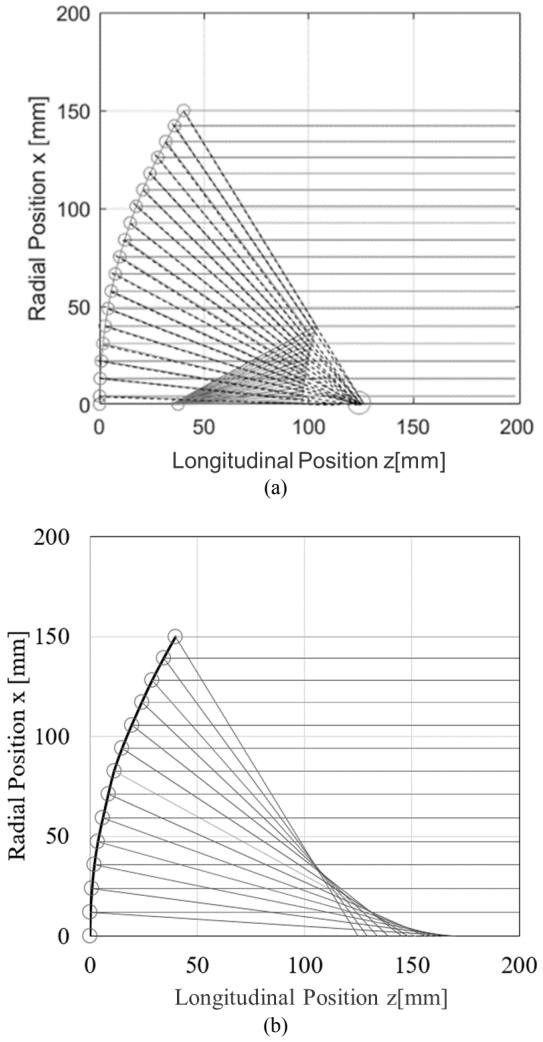

Fig. 17. The aperture distribution of $E_a^2(x)$ for (a) $p = 0$ and (b) $p = 1$.

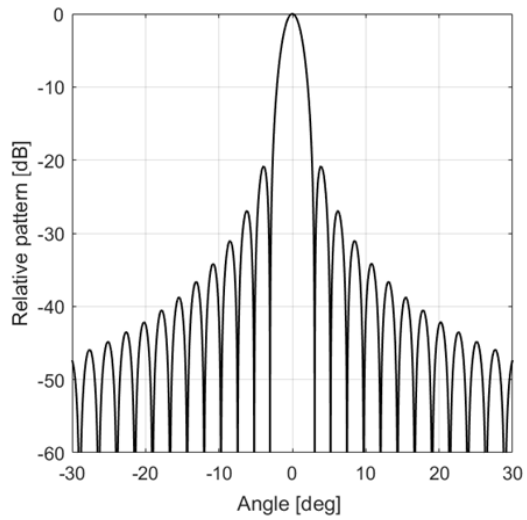

Fig. 18. Radiation pattern of the equivalent circle reflector.

4. Antenna Structure of Electromagnetic Simulation

4.1 Simulation Parameters

In order to obtain accurate radiation characteristics, such as antenna gain and multibeam radiation patterns of the equivalent parabola and circle reflectors, electromagnetic simulations are conducted by using a commercial software of FEKO. The simulation parameters are shown in Tab. 6 based on the structure of Fig. 19. As the main parameters, diameters of main and sub reflectors are 300 mm and 80 mm, respectively. The frequency is 28 GHz.

4.2 Feed Horn

The feed horn size is shown in Tab. 6. In Fig. 20(a) and (b), the structure of the feed horn antenna and the radiation pattern are shown, respectively. The radiation pattern indicates that the edge level of the sub reflector becomes –10 dB. On the other side, Figure 20(c) shows that the horn antenna return loss S_{11} is –30.9 dB at 28 GHz. It gives evidence that the simulated horn antenna is working well.

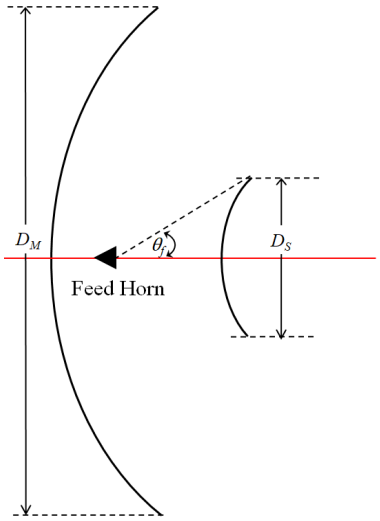

Fig. 19. Dual reflector structure.

Parameters	Value	Unit
Simulator	FEKO	
Method	PO	
Frequency (*Freq.*)	28	GHz
Diameter of main reflector (D_M)	300	mm
Diameter of sub reflector (D_S)	80	mm
The maximum feed angle (θ_t)	30	degree
Rectangular waveguide width of feed horn (*ww*)	7.5	mm
Rectangular waveguide length of feed horn (*wl*)	9	mm
Rectangular waveguide height of feed horn (*wh*)	6	mm
Flare width of feed horn (*hw*)	21	mm
Flare length of feed horn (*hl*)	20	mm
Flare height of feed horn (*hh*)	19	mm

Tab. 6. Electromagnetic simulation parameters.

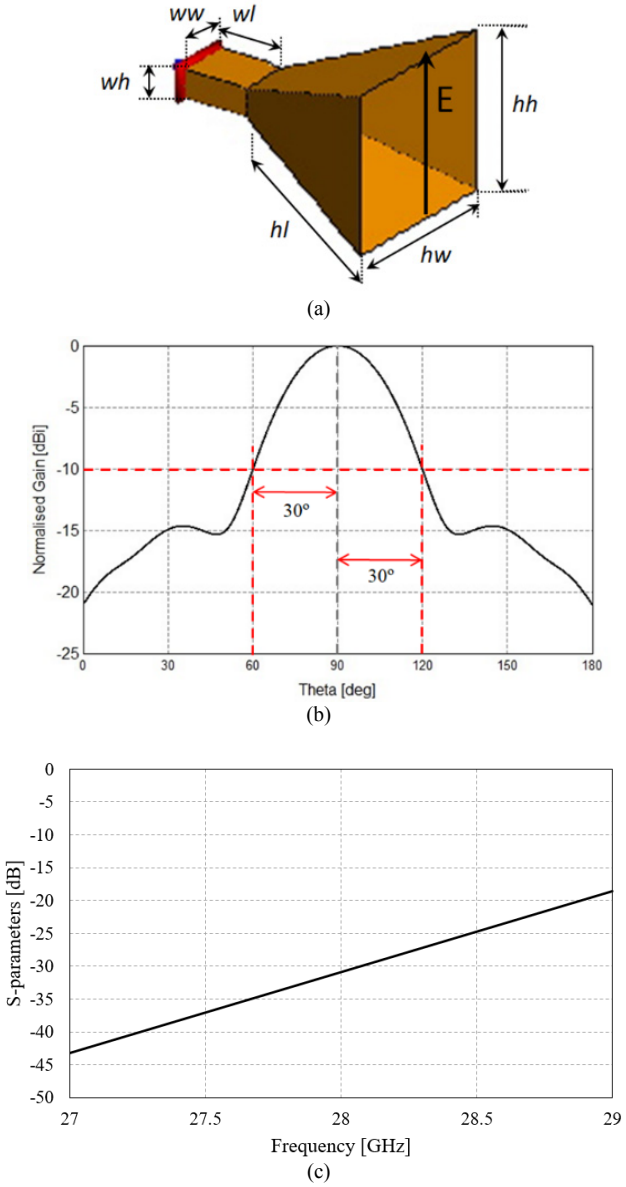

Fig. 20. (a) Structure, (b) the radiation pattern and (c) the return loss S_{11} of the feed horn

5. Simulation Results of Multibeam Radiation Patterns

5.1 Feed Position for Multibeam

In multibeam calculation, the feed position should be determined at the objective beam direction. The relation of the feed angle θ_F and beam direction angle θ_B are shown in Fig. 21. The ratio of θ_B to θ_F is called the beam deviation factor (BDF) as given by (23) [8].

$$BDF = \frac{\theta_B}{\theta_F} = \frac{1 + 0.36\left(\dfrac{D_M}{4f_{eq}}\right)^2}{1 + \left(\dfrac{D_M}{4f_{eq}}\right)}. \tag{23}$$

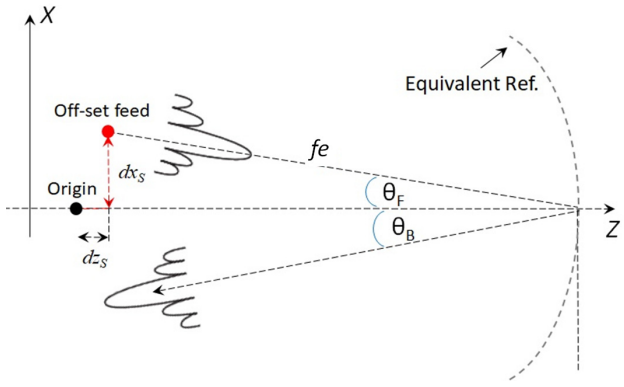

Fig. 21. Off-set feed position of the equivalent reflector.

Here, D_M is the main reflector diameter and f_{eq} is the focal length of the equivalent reflector [8].

Then, the displaced feed position (dx_s, dz_s) for the θ_B beam direction is given as follows:

$$dx_S = f_{eq} \sin\left(\frac{\theta_B}{BDF}\right), \tag{24}$$

$$dz_S = f_{eq} - f_{eq} \cos\left(\frac{\theta_B}{BDF}\right). \tag{25}$$

5.2 Multibeam Radiation Patterns of the Equivalent Parabola Method

Feed positions for beam angles θ_B are shown in Tab. 7. Here, f_{eq} is given by $f_e = 280$ mm of Tab. 2. The displaced feed positions and the radiation patterns for the beam angles of 0, 5, 10 and 15 degrees of the equivalent parabola method are shown in Figs. 22(a), (b), (c) and (d), respectively. It shows that the co-polarized components of the simulated designs which are represented by black solid line gradually reduce in accordance with the increase of the radiation angle and the beam widths increase in the off-axis beams. The cross-polarized components which are shown by the black dash line are –47.175 dB, –47 dB, –46.35 dB and –46 dB below the main beams of 0, 5, 10 and 15 degrees, respectively.

Figure 23 presents the return loss S_{11} of the equivalent parabola method for the beam angles of 0, 5, 10 and 15 degrees. Overall, it shows good return loss. Table 8 summarizes the simulated results of the equivalent parabola method in term of –10 dB beam width, the return loss S_{11}, gain and efficiency. Meanwhile, multibeam radiation patterns are shown in Fig. 24. It is found that the beam shape

Beam angle θ_B (degree)	Feed position (mm)	
	x_S	z_S
0	0	0
5	25	59
10	52	62
15	77	66

Tab. 7. Beam angle and off focus feed position of the equivalent parabola method.

degradation is rather fast for beam shift angle. At 15 degree beam shift angle, –10 dB beam width becomes 1.7 times larger than the center beam case. The reductions of gain and efficiency become 1.8 dB and 22%, respectively.

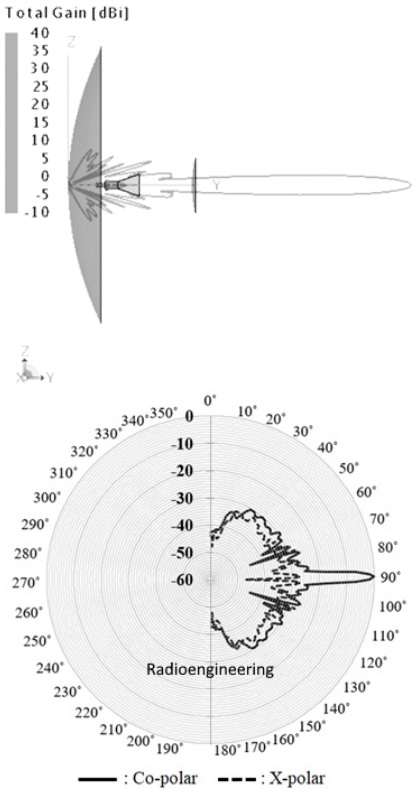

(a)

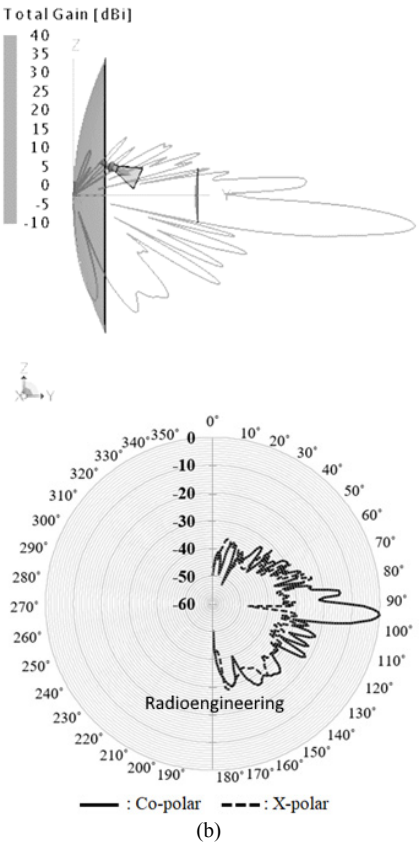

(b)

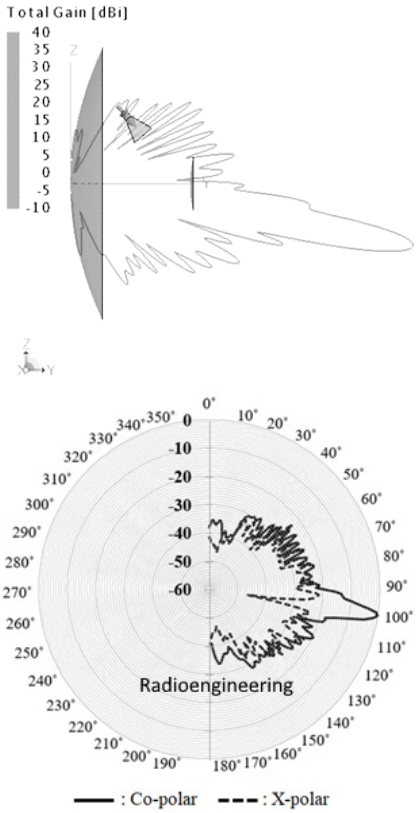

(c)

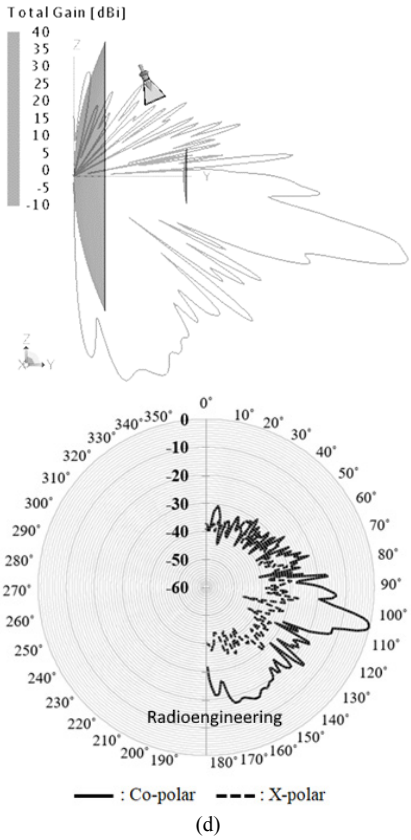

(d)

Fig. 22. Feed positions and radiation patterns for (a) On- axis, (b) 5 degree, (c) 10 degree and (d) 15 degree beams of the equivalent parabola method.

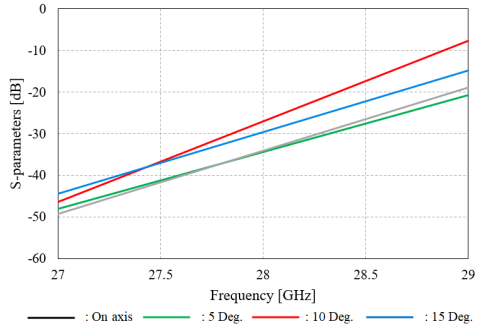

Fig. 23. The return loss S_{11} of the equivalent parabola method.

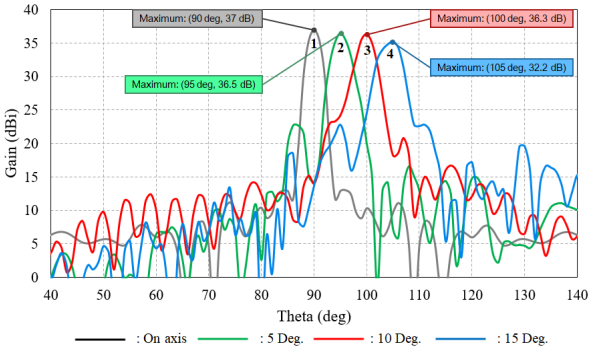

Fig. 24. Multibeam radiation patterns of the equivalent parabola method.

Beam angle θ_B (deg)	Beamwidth (deg)		S_{11} at 28 GHz (dB)	Gain (dBi)	Efficiency (%)
	–3 dB	–10 dB			
0	2.65	4.73	–34	37	64.6
5	3.5	6.7	–34.44	36.5	57.5
10	3.6	7.16	–27	36.2	53.7
15	4.8	8.2	–29.68	35.2	42.7

Tab. 8. Beamwidth, S_{11}, gain and efficiency of the equivalent parabola method.

5.3 Multibeam Radiation Patterns of the Equivalent Circle Method

Table 9 summarizes the feed positions for beam angles θ_B of the equivalent circle method. Here, f_{eq} is given by $f_c = 300$ mm as shown in Tab. 4. Figures 25(a), (b), (c) and (d) present the radiation patterns of the equivalent circle dual reflector antenna when the beam is scanned by 0, 5, 10 and 15 degrees, respectively. It is apparent that low levels of cross-polarization are obtained at 0 to 15 degrees beam scanning considered in this design. On the other side, the co-polarization of its electric field shows a smooth degradation in beam width.

Beam angle θ_B (degree)	Feed Position (mm)	
	x_s	z_s
0	0	0
5	23	35.5
10	46	38.5
15	69	43.5

Tab. 9. Beam angle and off focus feed position of the equivalent circle method.

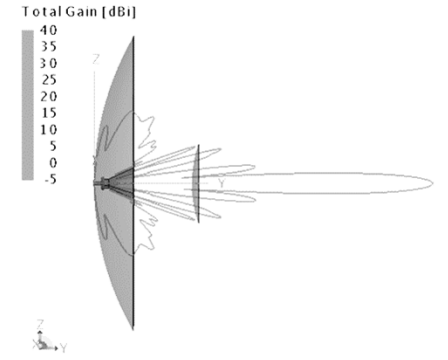

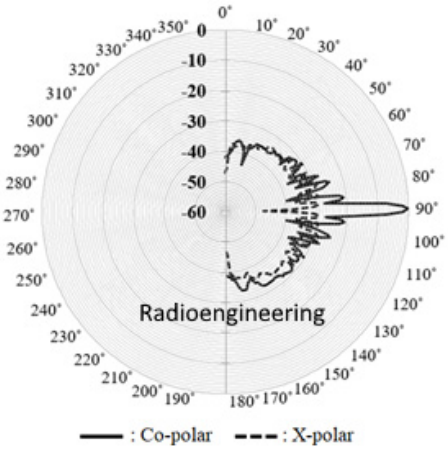

(a)

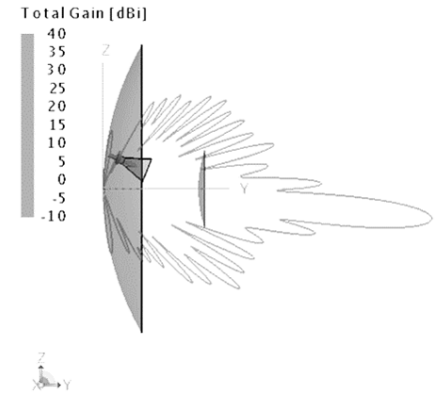

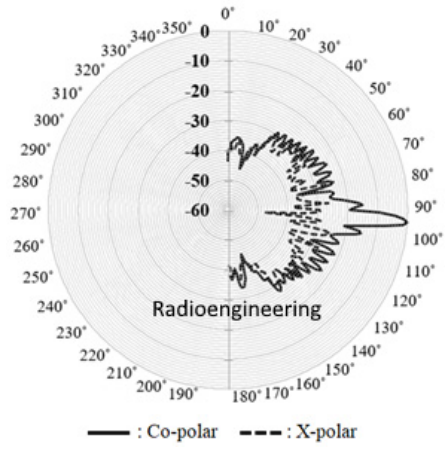

(b)

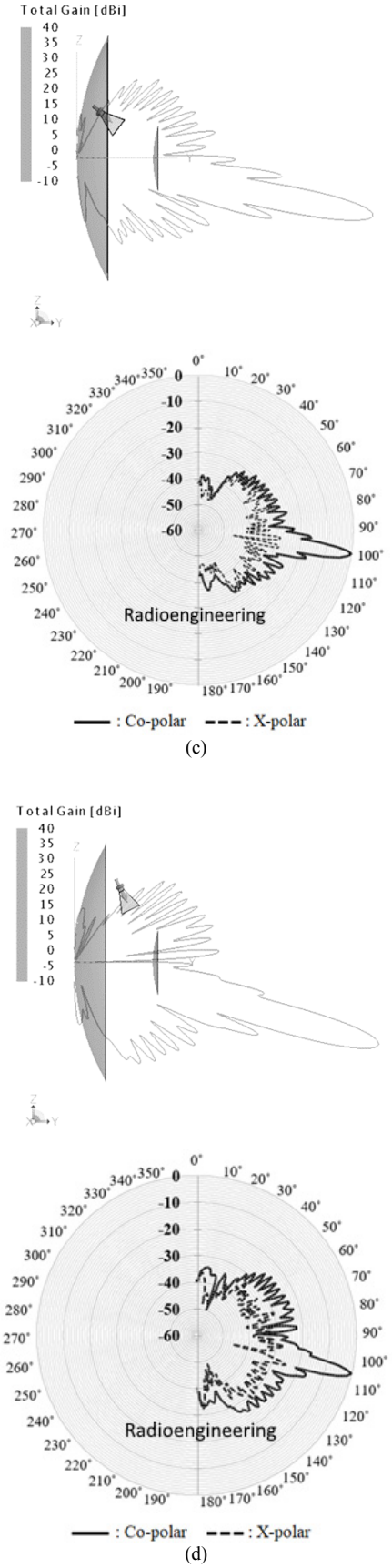

Fig. 25. Feed positions and radiation patterns for (a) On- axis, (b) 5 degree, (c) 10 degree, and (d) 15 degree beams of the equivalent circle method.

Figure 26 shows a plot of the return loss S_{11} versus frequency for this design where it is lower than –29 dB. The simulation results of the off-set feed equivalent circle dual reflector are summarized in Tab. 10. In addition, Figure 27 shows the multibeam radiation patterns for the equivalent circle method. The envelope of each beam gradually reduces in accordance with the increase of the radiation angle and the beam widths increase in the off-axis beams. It is clearly observed that the gain reduction at the 15 degrees off beam position is 1.2 dB, thus the efficiency is 16%. One interesting finding is a smooth degradation in gain that was found in the off axis feed configuration. This reduction is nearly related to the increment in the beam width of 1.4 times. It is interesting to note that these results show the proposed methods in this study can be adopted in designing circle dual reflector antenna configuration.

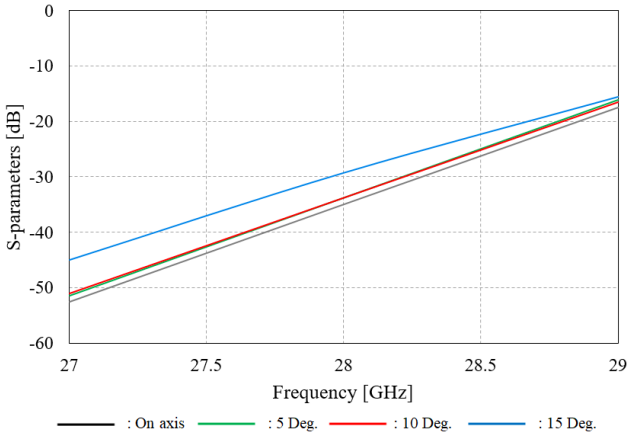

Fig. 26. The return loss S_{11} of the equivalent circle method.

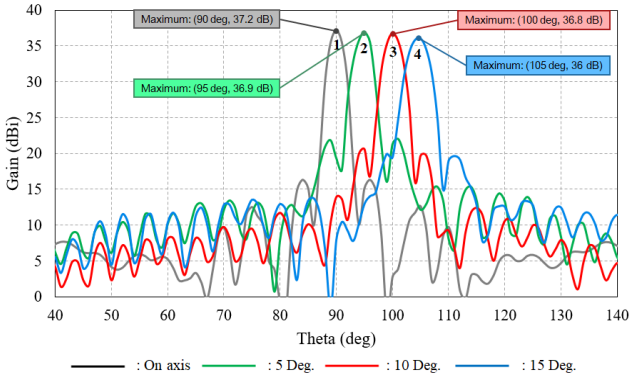

Fig. 27. Multibeam radiation patterns of the equivalent circle method.

Beam angle θ_B (deg)	Beamwidth (deg)		S_{11} at 28 GHz (dB)	Gain (dBi)	Efficiency (%)
	–3 dB	–10 dB			
0	2.6	4.64	–35	37.2	67.6
5	3.4	5.4	–33.8	36.9	63.1
10	3.5	6	–33.6	36.8	61.6
15	4.5	6.7	–29.3	36	51.3

Tab. 10. Beamwidth, S_{11}, gain and efficiency of the equivalent circle method.

5.4 Comparisons of Multibeam Characteristics between Equivalent Parabola and Circle Methods

Changes in antenna gain and beam shape for multibeam radiation patterns as shown in Figs. 23 and 26 are observed numerically. First, antenna gain comparisons are shown in Fig. 28. The remarkable thing is that the gains of the equivalent circle case become higher than the equivalent parabola case. Moreover, gain degradation for beam angle shift becomes smaller in the equivalent circle case.

As for the change in beam shape for multi beam operation, the associated beam widths at –3dB and –10dB levels are shown in Fig. 29. At –3dB beam width, any differences between the equivalent parabola and circle are not clear. At –10 dB beam width, significant differences are observed. In the equivalent circle case, the beam width changes from 4.6 deg to 6.7 deg for beam directions of 0 deg to 15 deg, respectively. The beam width expansion rate becomes 1.45. In the equivalent parabola case, the beam width changes from 4.7 deg to 8.2 deg for beam directions of 0 deg to 15 deg, respectively. The beam width expansion rate becomes 1.74. It is clarified that the beam shape change is suppressed to 1.45 of the equivalent circle case from 1.74 of the equivalent parabola case. It can be observed that by applying the equivalent circle equation to the conventional reflector shaping method, the gain reduction and beam shape degradation are reduced as compared to the equivalent parabola equation case.

Table 11 summarizes a comparison which is drawn between the results of the proposed dual reflectors in this paper and previous works on multibeam array antenna at frequency of 28 GHz [3–5] in order to demonstrate the potential of the proposed equivalent methods in this paper. It can be observed that the proposed equivalent parabola and circle reflectors are able to provide good performances compared to previous multibeam array antennas in terms of S_{11} and gain. The proposed reflectors based on the equivalent parabola and circle shaping methods have a slight maximum gain drop compared to others.

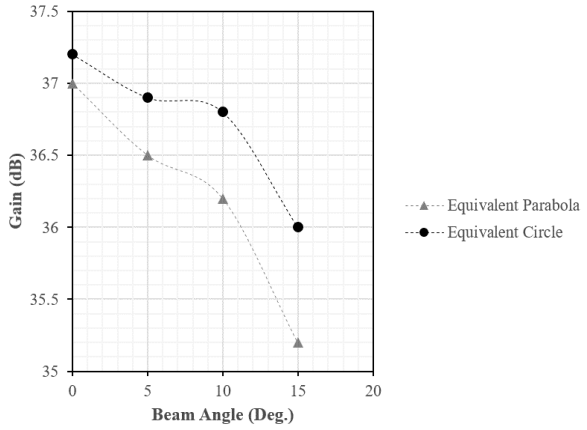

Fig. 28. Gain variation with changing the off beam angle for the equivalent parabola and circle dual reflectors.

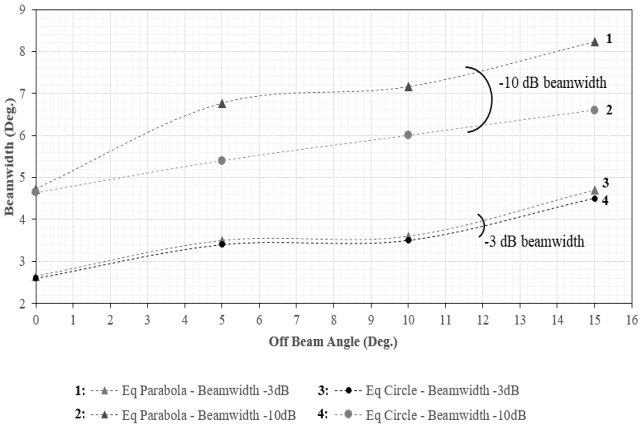

Fig. 29. Beam width change of the equivalent parabola and circle reflectors.

Reference	S_{11} at 28 GHz (dB)	Maximum gain (dBi)	Minimum gain (dBi)
[3]	–15	16	11
[4]	–14	15.2	9.2
[5]	–16	24.4	20.9
The proposed equivalent parabola reflector	–34	37	35.2
The proposed equivalent circle reflector	–35	37.2	36

Tab. 11. Beamwidth, S_{11}, gain and efficiency of the equivalent circle method.

6. Conclusion

New reflector shaping methods using the equivalent parabola equation and the equivalent circle equation are proposed. First, reflector shape design program was developed by MATLAB software for conventional shaping method to ensure the reliability of the program performance. Next, the conventional shaping program was modified for the equivalent parabola and circle reflectors. The calculated ray tracing results, reflector shapes, aperture distributions and radiation patterns of the three reflector shaping methods have shown the accuracy of the MATLAB program. Moreover, comparisons of the MATLAB results with electromagnetic simulation results were done and good agreement has been obtained. The off-beam characteristics of equivalent parabola and circle dual reflectors were investigated through FEKO simulator. In the equivalent circle case, high aperture efficiency of 67.6% has been achieved. As for multibeam characteristics, gain reduction at 15 degree beam was small, which is only 1.2 dB. Small beam shape change ratio of 1.45 was also achieved. In the equivalent parabola case, aperture efficiency is 64.6%. As for multibeam characteristics, the gain reduction at 15 degree beam is 1.8 dB and the beam shape change ratio is 1.74. For all parameter values of aperture efficiency, beam gain reduction and beam shape change, the equivalent circle reflector becomes superior. As a result, it is ensured that high gain and good multibeam radiation patterns can

be achieved by applying the equivalent circle equation to the conventional reflector shaping method.

Acknowledgments

This research was funded by Universiti Teknologi Malaysia (UTM) and the Ministry of Education (MOHE), with grant number of 5F046.

References

[1] SHHAB, L., RIZANER, A., ULUSOY, A. H., et al. Suppressing the effect of impulsive noise on millimeter-wave communications systems. *Radioengineering,* 2020, vol. 29, no. 2, p. 376–385. DOI: 10.13164/re.2020.0376

[2] XIE, Y., LI, B., YAN, Z., et al. A general hybrid precoding method for mmwave massive MIMO systems. *Radioengineering,* 2019, vol. 28, no. 2, p. 439–446. DOI: 10.13164/re.2019.0439

[3] ZHONG, L. H., BAN, Y. L., LIAN, J. W., et al. Miniaturized SIW multibeam antenna array fed by dual-layer 8x8 Butler matrix. *IEEE Antennas and Wireless Propagation Letters*, 2017, vol. 16, p. 3018–3021. DOI: 10.1109/LAWP.2017.2758373

[4] IDRUS, I. I., ABDUL LATEF, T., ARIDAS, N. K., et al. Design and characterization of a compact single-layer multibeam array antenna using an 8×8 Butler matrix for 5G base station applications. *Turkish Journal of Electrical Engineering and Computer Sciences,* 2020, vol. 28, p. 1121–1134. DOI: 10.3906/elk-1907-119

[5] ISHFAQ, M. K., ABD RAHMAN, T., YOSHIHDE, Y., et al. 8×8 phased series fed patch antenna array at 28 GHz for 5G mobile base station antennas. In *Proceedings of 2017 IEEE-APS Topical Conference on Antennas and Propagation in Wireless Communications (APWC)*. Verona (Italy), 2017, p. 160–162. DOI: 10.1109/APWC.2017.8062268

[6] AHSAN, M. R., ISLAM, M. T., YAMADA, Y., et al. Ray tracing technique for shaping a dual reflector antenna system. *Turkish Journal of Electrical Engineering and Computer Sciences*, 2016, vol. 24, no. 3, p. 1223–1234. DOI: 10.3906/elk-1311-214

[7] ISHIMARU, A., SREENIVASIAH, I., WONG, V. Double spherical Cassegrain reflector antennas. *IEEE Transactions on Antennas and Propagation*, 1973, vol. 21, no. 6, p. 774–780. DOI: 10.1109/TAP.1973.1140607

[8] QUZWAIN, K., YAMADA, Y., KAMARDIN, K., et al. Reflector surface shaping method for a Cassegrain antenna. In *Proceedings of the 6th International Conference on Space Science and Communication (IconSpace)*. Johor Bahru (Malaysia), 2019, p. 207–211. DOI: 10.1109/IconSpace.2019.8905935

[9] STUTZMAN, W. L., THIELE, G. A. *Antenna Theory and Design*. 3rd ed. New York (USA): John Wiley, 2012. ISBN: 1118213475

[10] BALANIS, C. A. *Antenna Theory: Analysis and Design.* 2nd ed. New York (USA): John Wiley, 1996. ISBN: 978-0471592686

[11] ZAMAN, M. A, ABD MATIN, MD. A new method of designing circularly symmetric shaped dual reflector antennas using distorted conics. *International Journal of Microwave Science and Technology*, 2014, vol. 2014, p. 1–8. DOI: 10.1155/2014/849194

[12] SPANCER, R. C., HYDE, G. Studies of the focal region of a spherical reflector: Geometric optics. *IEEE Transactions on Antennas and Propagation*, 1968, vol. 16, no. 3, p. 317–324. DOI: 10.1109/TAP.1968.1139187